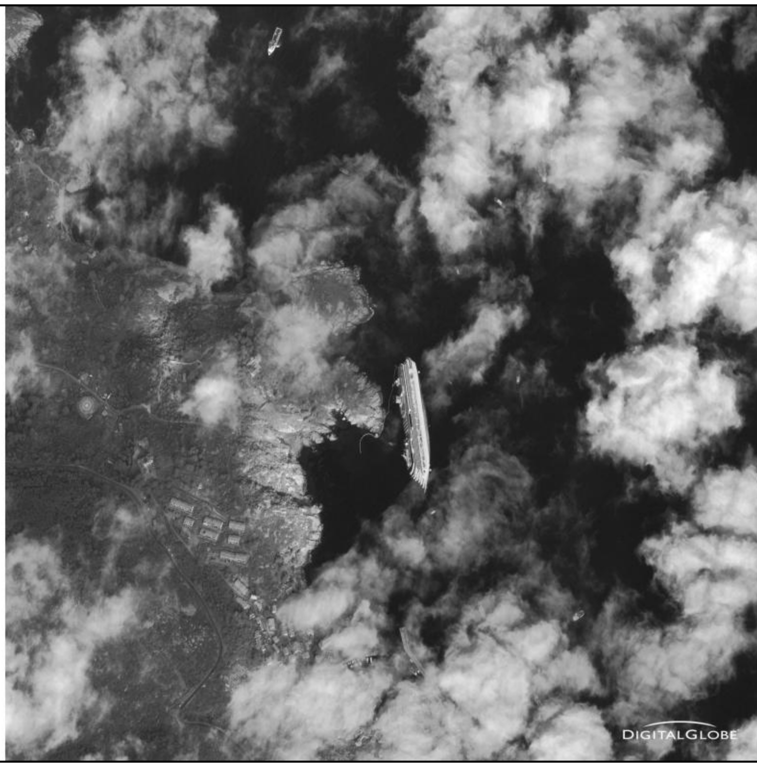
DIGITALGLOBE

Spectroscopy of Plant Canopies Chapter 11, 2, 7

Leaf area index, leaf angle distribution
Landscape components, structure
Digital Multispectral (MSS, Landsat, SPOT)
Orbital configurations

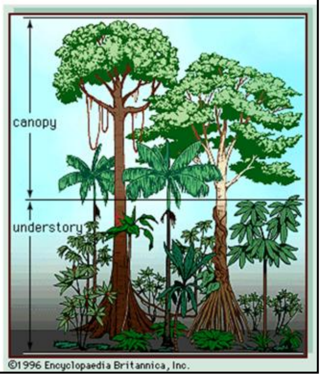

Daintree Biosphere Reserve, Queensland, Australia

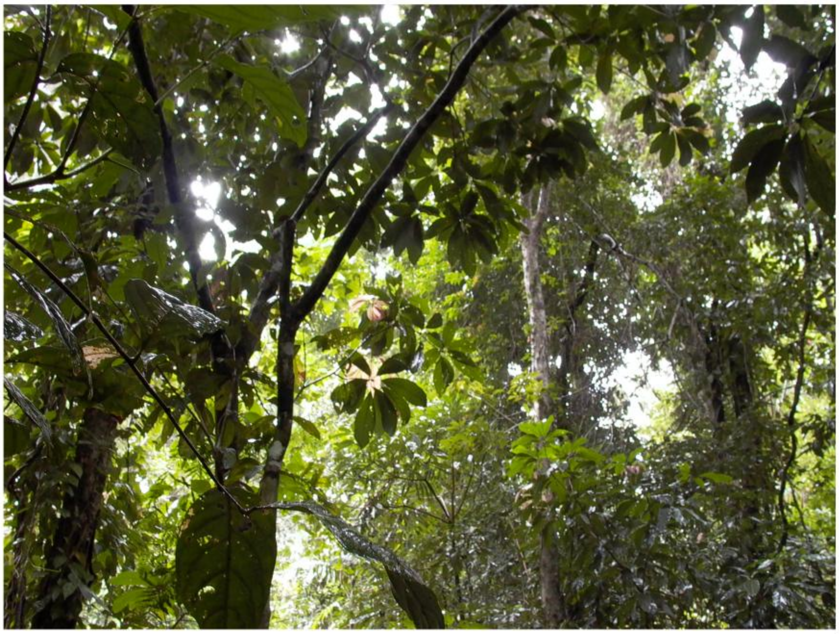

3

What do you see when you look up through a canopy that indicates how the ecosystem is functioning?

Light is transmitted, absorbed and reflected

Three factors determine reflectance at canopy scale

1. **Absorbing properties of canopy components: leaves, stems, flowers, fruit, soil background, etc.**
   - absorption by plant biochemicals (pigments, water, CHO)
   - absorption by soil biogeochemicals (soil minerals and clays)
   - Transmission through canopy
2. **Canopy architecture.**

   (scattering by: above-ground biomass; modified by leaf area index and arrangement of foliage and branches in space (x,y,z and zenith, azimuth position of sun)
   - Leaf, stem, branch orientations in space
   - plant spacing and orientation (random, rows, regular)
   - Composition of species within a pixel
   - Soil background, topography, roughness
3. **Directions of illumination and view.**
   - direct and diffuse radiation
   - position of detector
   - irradiance and exitance
   - bidirectional reflectance distribution function

Influence of Wood & *Litter on Canopy Reflectance

SAI: Stem Area Index

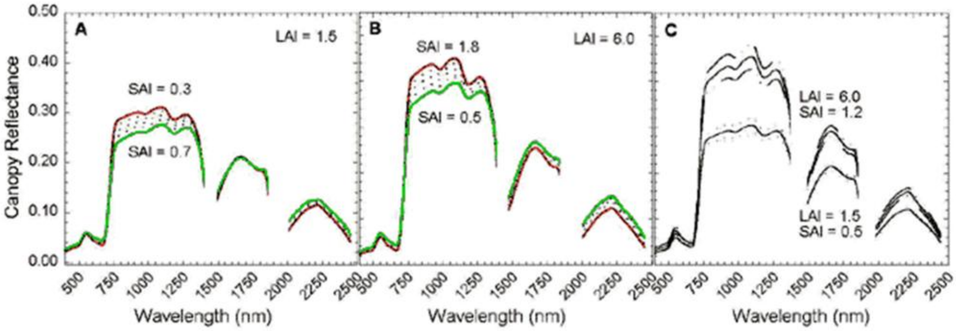

- Amount of woody matter influences NIR reflectance (Asner, 1998)
- Knowledge of the dry biomass is key to estimating plant/ecosystem. respiration, a component of biogeochemical cycling.
- Biomass is used to estimate carbon storage, fuel loads for wildfire risk, etc.

*Plant litter ("residue"): dry stems, leaves, and woody stems

Wind River Canopy
Crane Site, Carson, WA

500 yr "old growth"
Conifer Forest

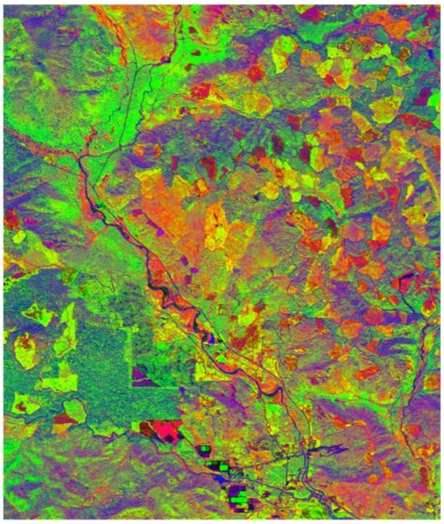

R= soil, G=vegetation, B=shade

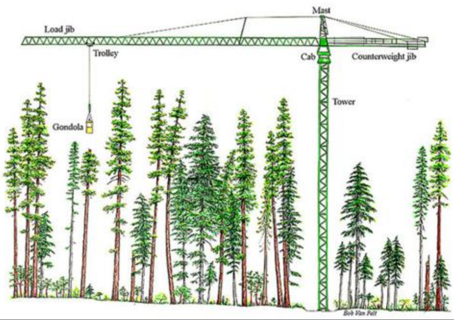

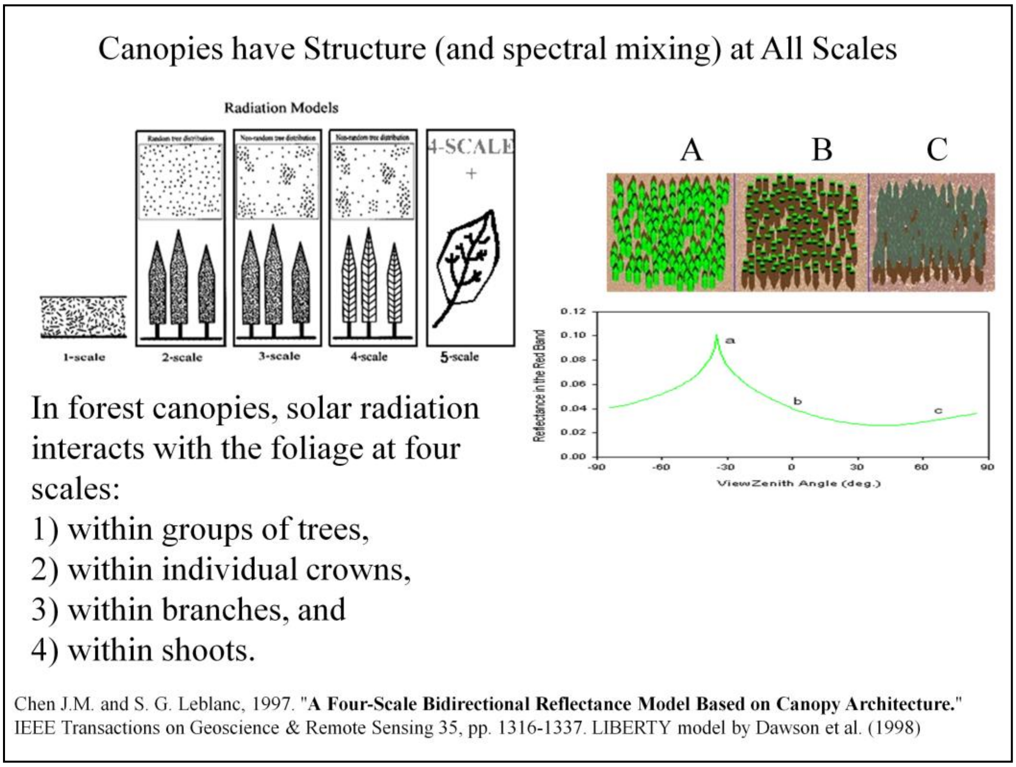

1-scale: turbid media;
2-scale: randomly distributed discrete objects containing turbid media;
3-scale: non-random discrete objects containing turbid media; and
4-scale: non-random discrete objects with internal structures (such as branches and shoots).

5-scale: leaf biochemistry and anatomy (4-scale + RT leaf model)

a) backward scattering, where the sun and the viewer are on the same side, hiding most of the shadows;
(**b**) nadir view, where a maximum of the background can be seen; and
(**c**) forward scattering where the sun and the viewer are on the opposite side.

Leaf Reflectance and Transmission Measurements and Calculated Absorptance

POTR: Populus trichocarpa (cottonwood)

ACMA: Acer macrophyllum (bigleaf maple)

ALRU Alnus rubra (red alder)

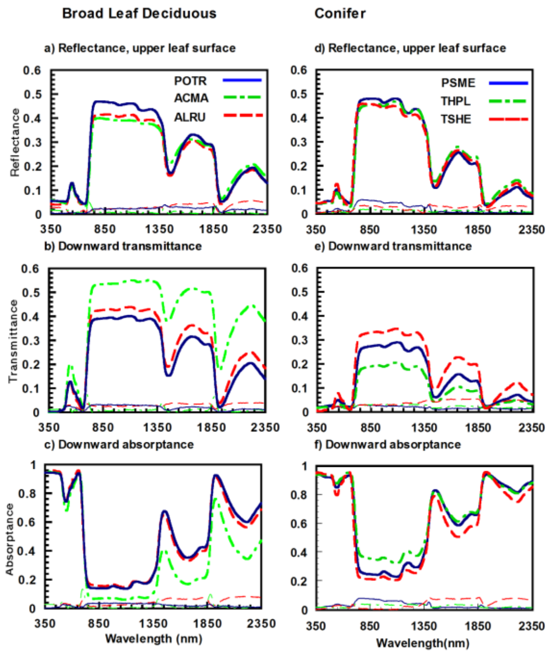

PSME: Pseudotsuga menziesii (Douglas Fir)

THPL: Thuja plicata (Western Redcedar)

TSHE: *Tsuga heterophylla* (western hemlock)

Roberts, D.A., S.L. Ustin, S. Ogunjemiyo, J. Greenberg, S.Z. Dobrowski, J. Chen, and T.M. Hinckley. 2004. Spectral and structural measures of northwest forest vegetation at leaf to landscape scale. Ecosystems 7 (5): 545-562

Leaf-level hemispherical reflectance and transmittance spectra of three broadleaf and three conifer dominants. Reflectance is plotted as a solid line; transmittance, as a dashed line. Plots show the mean ± SD. Species names follow the codes in the text. POTR, *Populus trichocarpa*; ACMA, *Acer macrophyllum*; ALRU, *Alnus rubra*; PSME, *Pseudotsuga menziesii*; THPL, *Thuja plicata*; TSHE, *Tsuga heterophylla*.

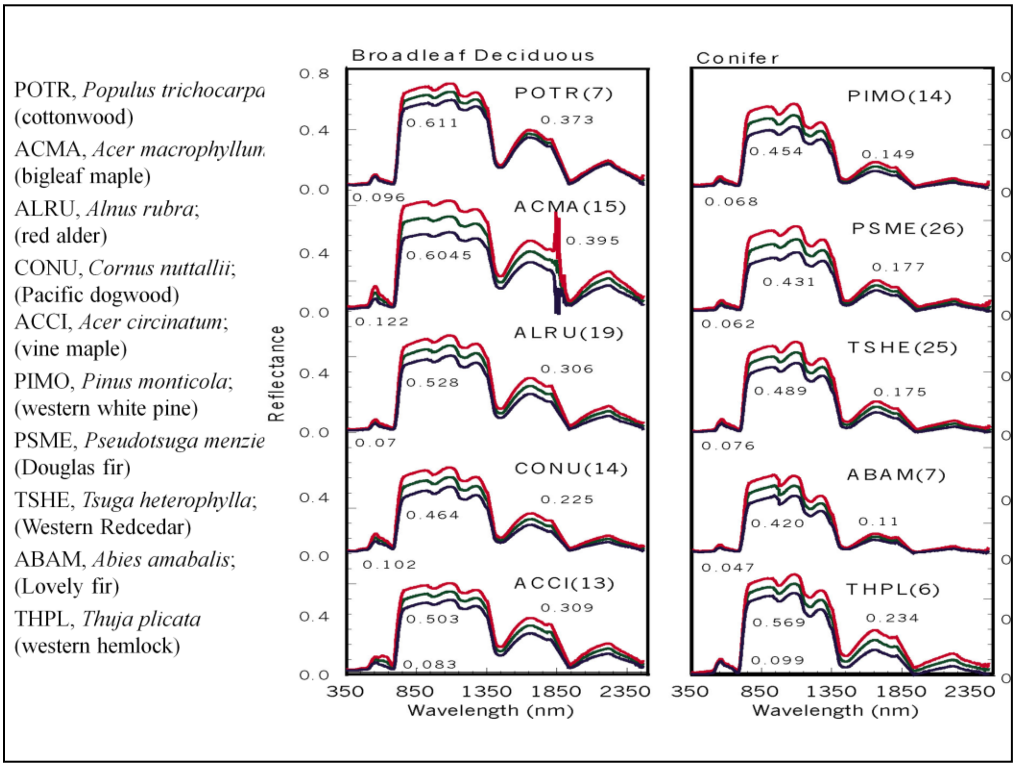

Branch-scale reflectance spectra of five broadleaf deciduous species and five conifer species. Plots show the mean ± SD. The number of spectra used in the average is shown in parentheses. Numbers shown beside each plot correspond to reflectance at 550, 830, and 1,650 nm (in the green, near-infrared (NIR), and short-wave infrared (SWIR) spectral regions, respectively). POTR, *Populus trichocarpa*; ACMA, *Acer macrophyllum*; ALRU, *Alnus rubra*; CONU, *Cornus nuttallii*; ACCI, *Acer circinatum*; PIMO, *Pinus monticola*; PSME, *Pseudotsuga menziesii*; TSHE, *Tsuga heterophylla*; ABAM, *Abies amabalis*; THPL, *Thuja plicata*.

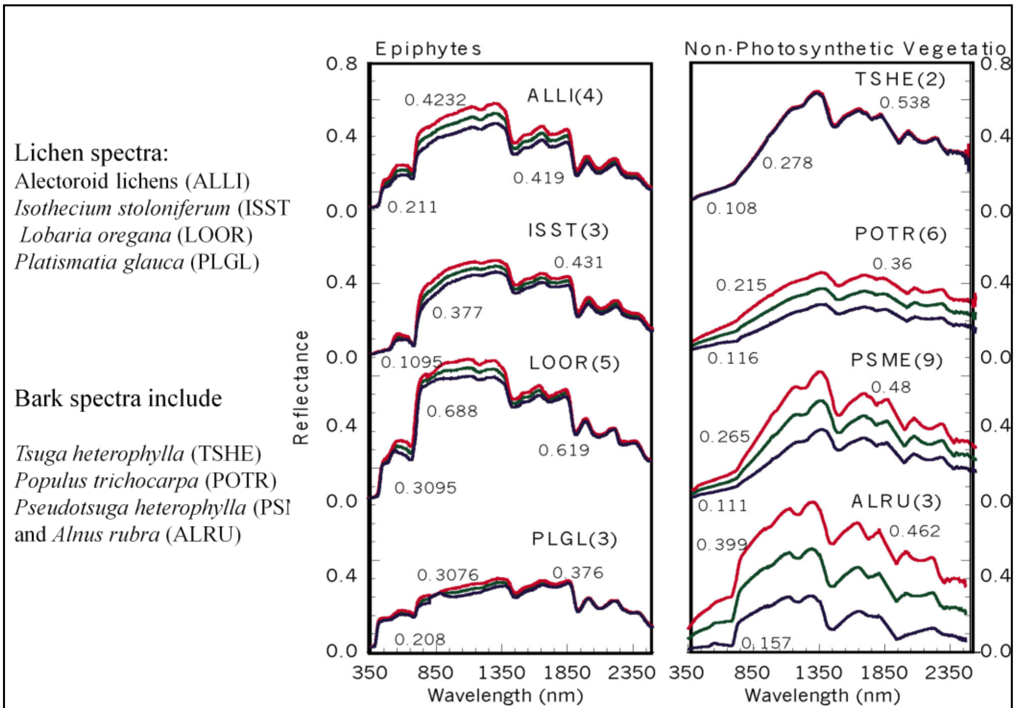

Roberts, D.A., S.L. Ustin, S. Ogunjemiyo, J. Greenberg, S.Z. Dobrowski, J. Chen, and T.M. Hinckley. 2004. Spectral and structural measures of northwest forest vegetation at leaf to landscape scale. Ecosystems 7 (5): 545-562

Branch-scale reflectance spectra of four nonvascular epiphytes and four types of nonphotosynthetic vegetation (NPV). Plots show the mean ± SD (above and below the mean). The number of spectra used in the average is shown in parentheses. Epiphyte spectra include an assemblage of Alectoroid lichens (ALLI), *Isothecium stoloniferum* (ISST), *Lobaria oregana* (LOOR), and *Platismatia glauca* (PLGL). Bark spectra include *Tsuga heterophylla* (TSHE), *Populus trichocarpa* (POTR), *Pseudotsuga heterophylla* (PSME), and *Alnus rubra* (ALRU). Numbers shown beside each plot correspond to reflectance at 550, 830, and 1,650 nm (green, near-infrared (NIR), and short-wave infrared (SWIR) spectral regions, respectively).

(a)Stand-scale reflectance spectra of a very recently regenerated clearcut

(**b, c, d, e**) age classes of *Pseudotsuga menziesii* (PSME)

(f) Mixed 80-year-old stand of PSME and TSHE)

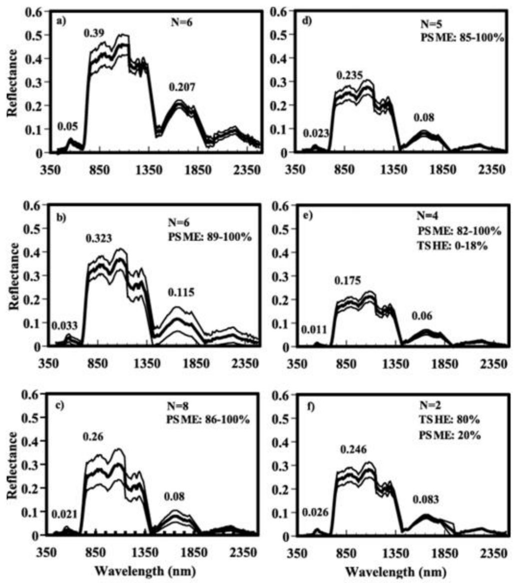

Roberts, D.A., S.L. Ustin, S. Ogunjemiyo, J. Greenberg, S.Z. Dobrowski, J. Chen, and T.M. Hinckley. 2004. Spectral and structural measures of northwest forest vegetation at leaf to landscape scale. Ecosystems 7 (5): 545-562

Stand-scale reflectance spectra of a very recently regenerated clearcut (**a**), four age classes of *Pseudotsuga menziesii* (PSME) (**b–e**), and an 80-year-old *Tsuga heterophylla* (TSHE) stand (**f**). Plots show the mean ± SD (above and below the mean). The number of spectra used in the average is shown.

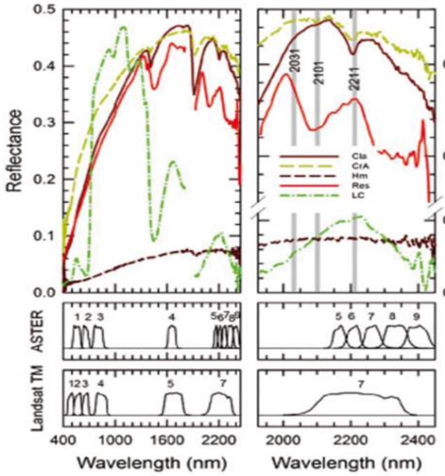

$$CAI = 0.5\,(R_{2000} - R_{2200})/R_{2100}$$

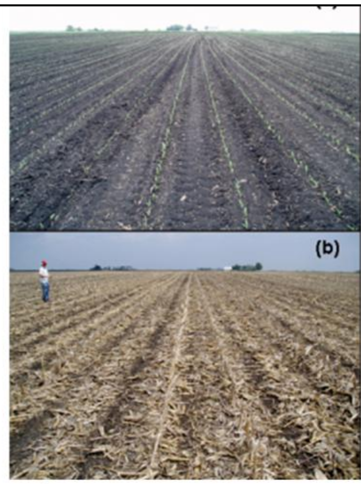

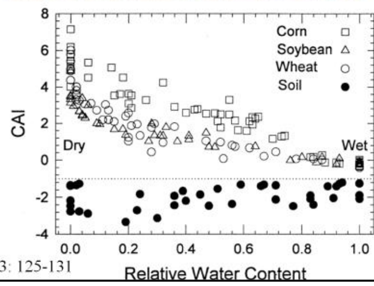

Craig S.T. Daughtry. 2001. Agronomy Journal 93: 125-131

Absorption by Water Vapor, Liquid and Solid Phases in the Solar Reflected Spectrum

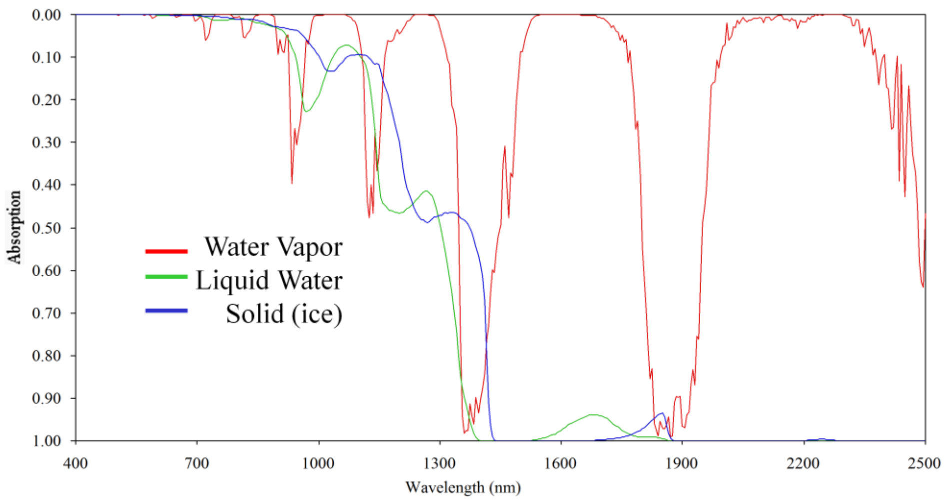

Near 1000 nm absorption spectra for three phases of water overlap but maxima are displaced by wavelength

Robert O. Green

Note that near 1000 nm, that the wavelength of maximum absorption for water vapor is at the shortest wavelength, then liquid water and frozen water at the longest wavelength.

Santa Monica Mtns: Canopy Water Content

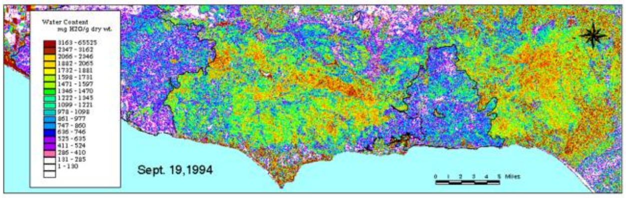

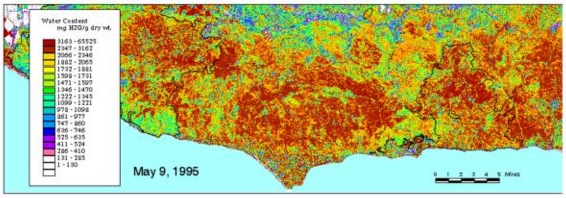

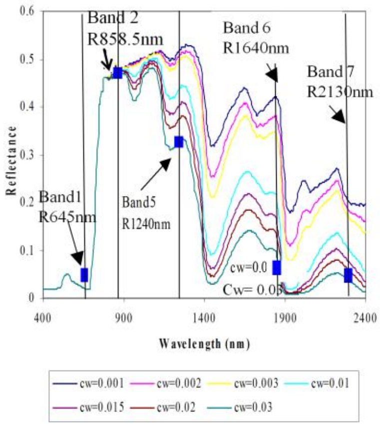

Ustin et al., Photonics, 1999

Modeled with PROSPECT, adapted from Zarco-Tejada et al. (2003)

Differences in Leaf Area Index (LAI)
LAI= m^2 leaf area/m^2 ground area

Relationship between LAI and canopy reflectance depends on:

- species
- age/growth
- scale of measurement
- Leaf area/leaf mass
- distribution of leaves in a crown
- leaf angle distribution
- many other factors

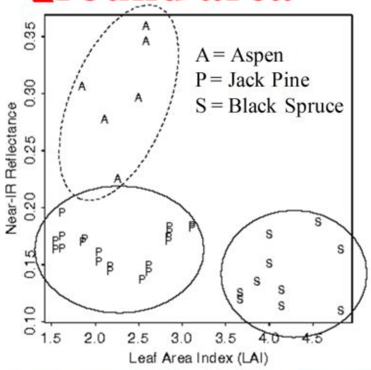

Aspen (fall) Jack Pine Black Spruce

Red and NIR Reflectance for:

(a) Different Canopy Densities (b) Change During a Growing Season

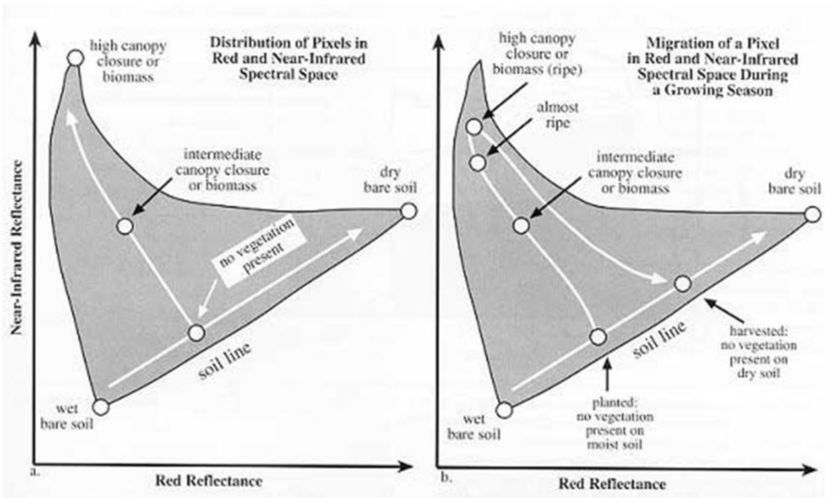

Plant Canopies Change with Growth over the Growing Season
(=Phenological Development)

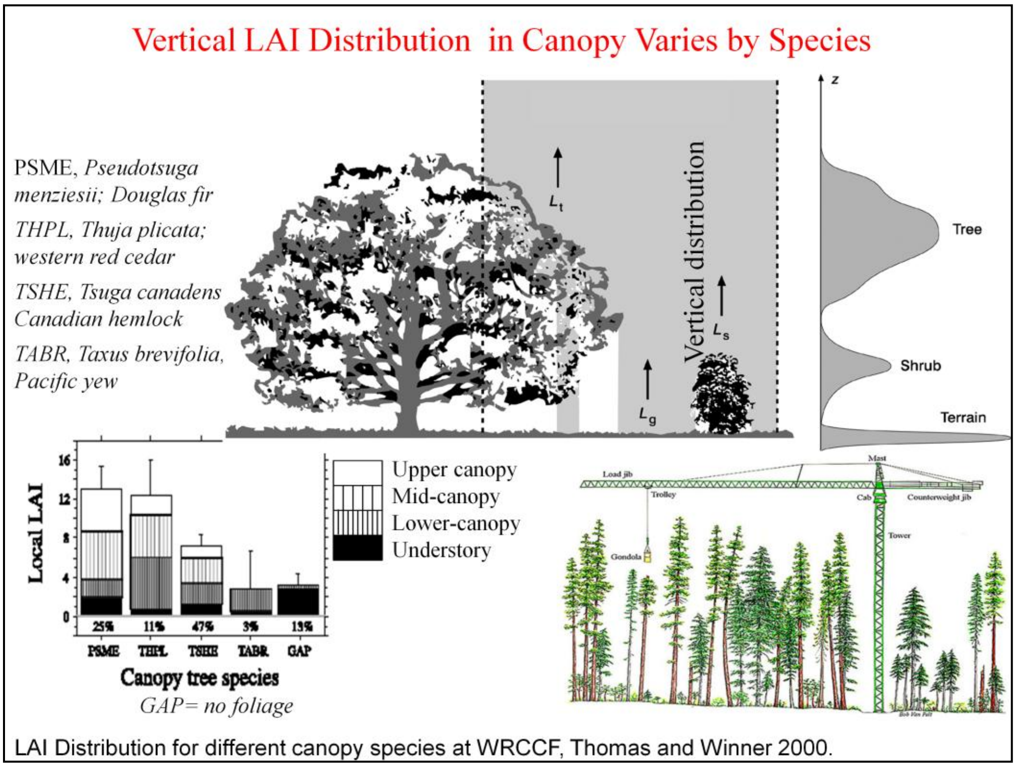

Fig. 2. Local LAI as a function of the uppermost tree species encountered, estimated on the basis of pooled vertical line intercept data at the Wind River Canopy Crane site (PSME, *Pseudotsuga menziesii; THPL, Thuja plicata; TSHE, Tsuga canadensis; TABR, Taxus brevifolia; GAP, no mid- or uppercanopy* foliage encountered). Shading corresponds to canopy layer, arranged from bottom to top as understory, lower-canopy, mid-canopy, and upper-canopy foliage. The proportions of sample points within each category are listed below each bar.

Canopy Reflectance Varies with Leaf Density (Leaf Area Index)

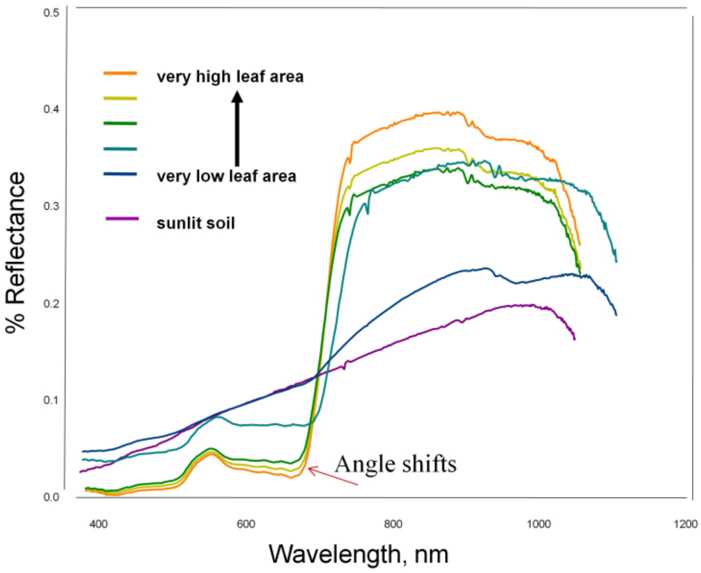

Red and NIR reflectance Varies with Leaf Area Index

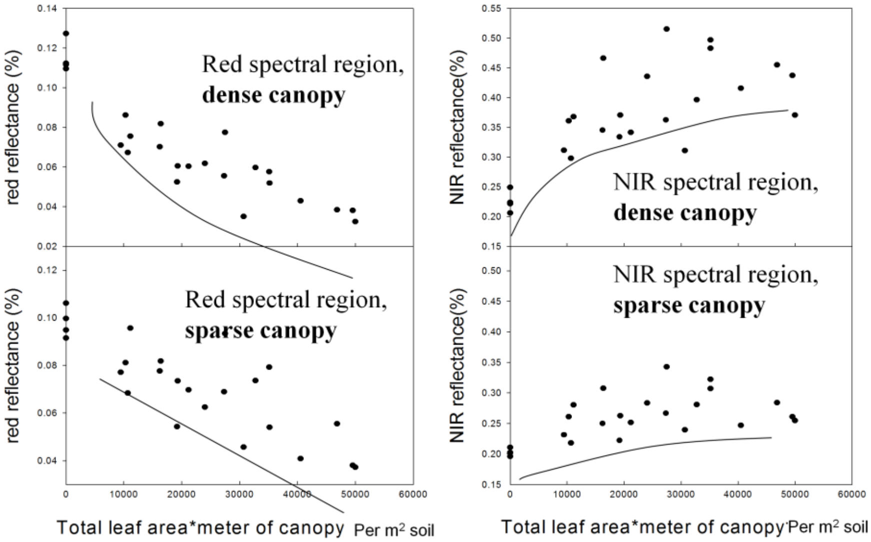

LAI = leaf area * m^{-2}, area of canopy

Note that red and NIR vary independently and that the response pattern isn't the same (e.g., linear) for low vegetation cover as for high vegetation cover.

What Happens to Light that is Transmitted Through a Turbid Medium?

Single vs. Multiple Scattering

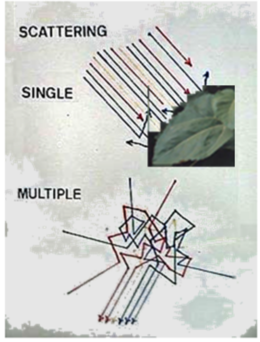

A. Single scattering occurs when light is absorbed or reflected on its first pass through the medium and doesn't interact after the first contact

B. Multiple scattering requires some transmittance through the medium

In plants, multiple scattering occurs where multiple leaf layers exist, such as in a dense plant canopy.
In geologic materials, when light passes through crystals, e.g., multiple sand grains

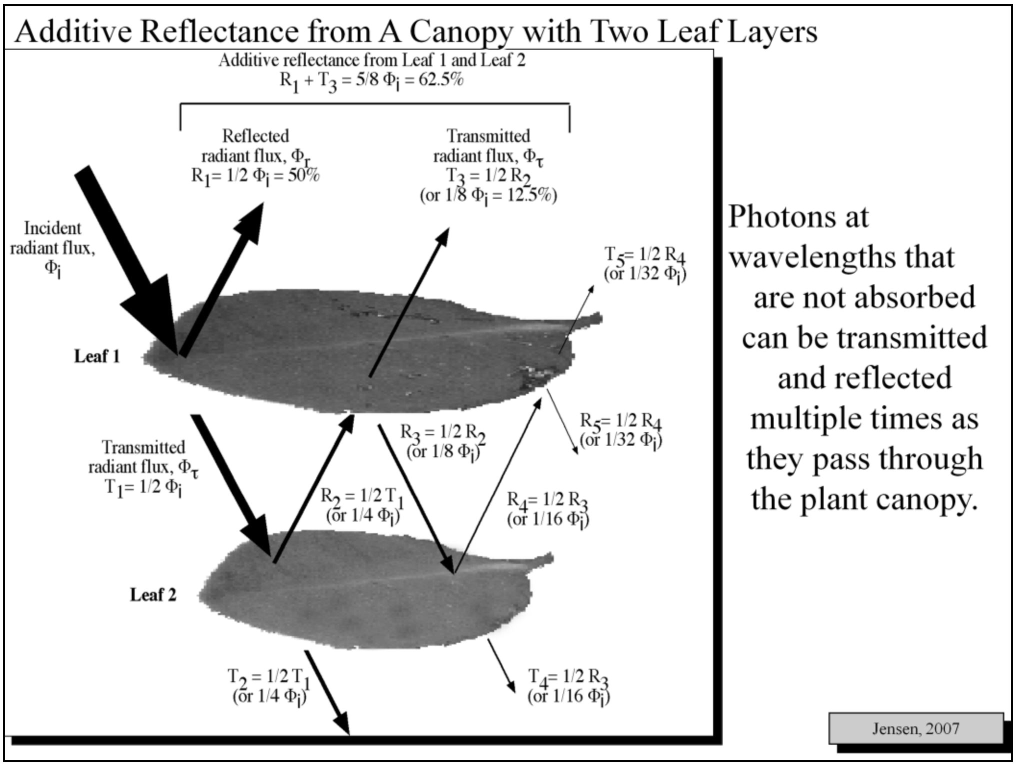

Assume that for each surface interaction ½ of the radiant flux is reflected and ½ transmitted and none is absorbed.

So, on the first pass, half is transmitted to leaf 2 and of that ½ is reflected (1/4 of incident flux) to the underside of leaf 1. Of this ½ (or 1/8 of the incident flux) is again reflected and ½ transmitted which is now 1/8 of the original incident flux, the last part of the flux to interact with both leaves is at the level of 1/32 reflected to leaf 1. If you add each of these reflectance components from the surface of leaf 1, it is equal to 1/2 + 1/8 + 1/32 = 21/32 = 65.625% of the total indicent radiant flux is reflected from the surface. And the rest is lost in transmission.

When light is scattered multiple times within the canopy the scattering becomes non-linear in proportion to the leaf area.

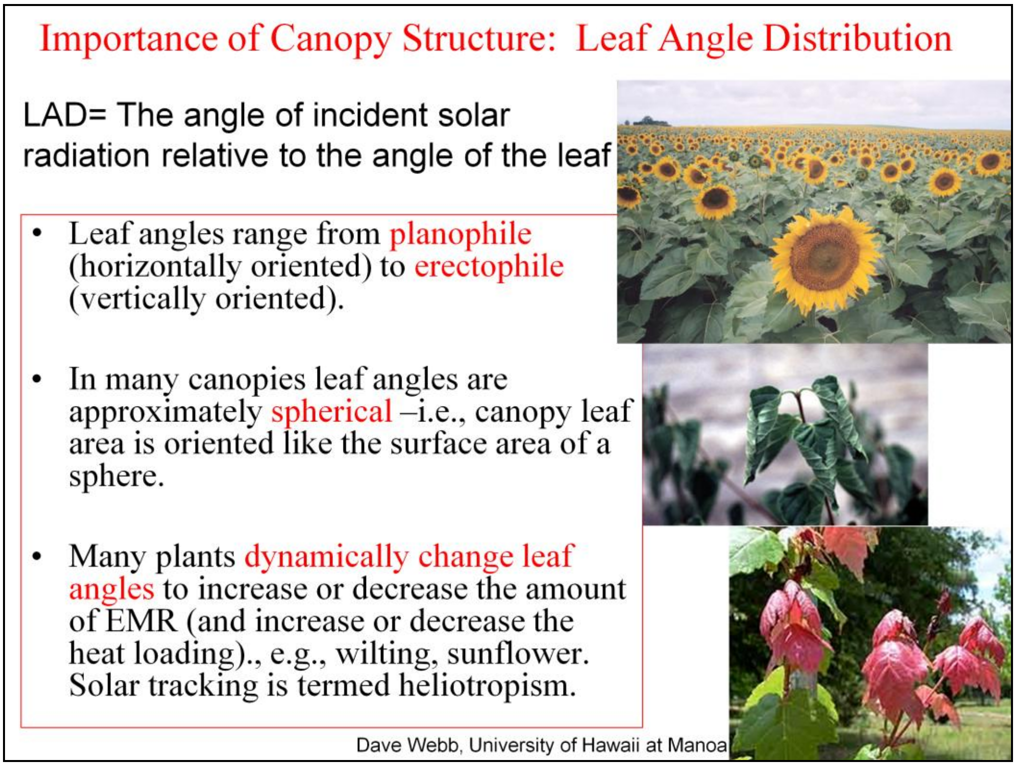

The LAD of a plant canopy has a significant impact on the reflectance, transmittance and absorption of solar light in the vegetation layer, and thus also on its growth and development. LAD can also serve as a quantitative index to monitor the state of the plants, as wilting usually results in more erectophile LADs. Models of radiation transfer need to take this distribution into account to predict, for instance, the albedo or the productivity of the canopy.

Both LAI & Leaf Angle Distribution (LAD) Affect Reflectance

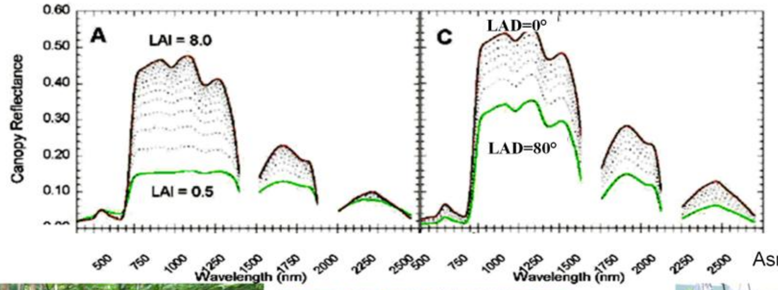

Asner, 1998

Planophile = ~0°

Erectophile = ~90°

Spherical leaf distribution
All angles

Extremes of Canopy Leaf Angle Distribution

Probability Distribution for Different LAD Types

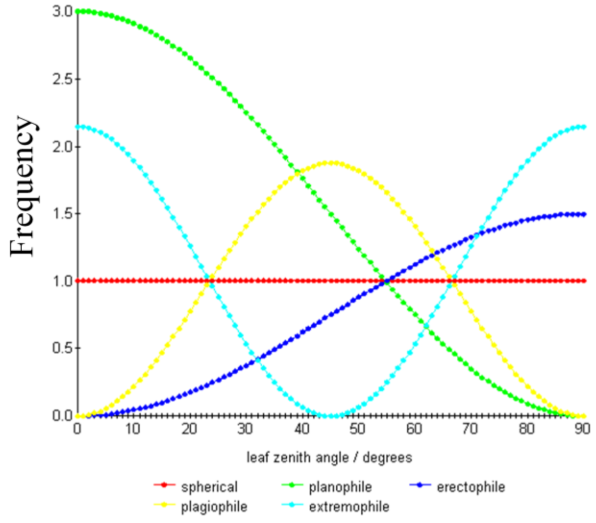

Planophile (foliage (horizontally dominated)

www.biologie.uni-hamburg.de/

Understory foliage

Giant arum in Costa Rica rainforest

Ligularia reniformus


Erectophile: Norfolk
Pine in high sunlight


Erectophile: Banana

Eucalyptus

Erectophile foliage (vertical)

Japanese Blood Grass

Imperiata cylndrica "Rubra"

Tule marsh (*Scirpus californicus*) canopies of the Sacramento Valley and delta have nearly vertical orientation.

Plagiophile: leaves at 45°

New Zealand Tree Fern

Spherical Distribution

Agave Eggersiana

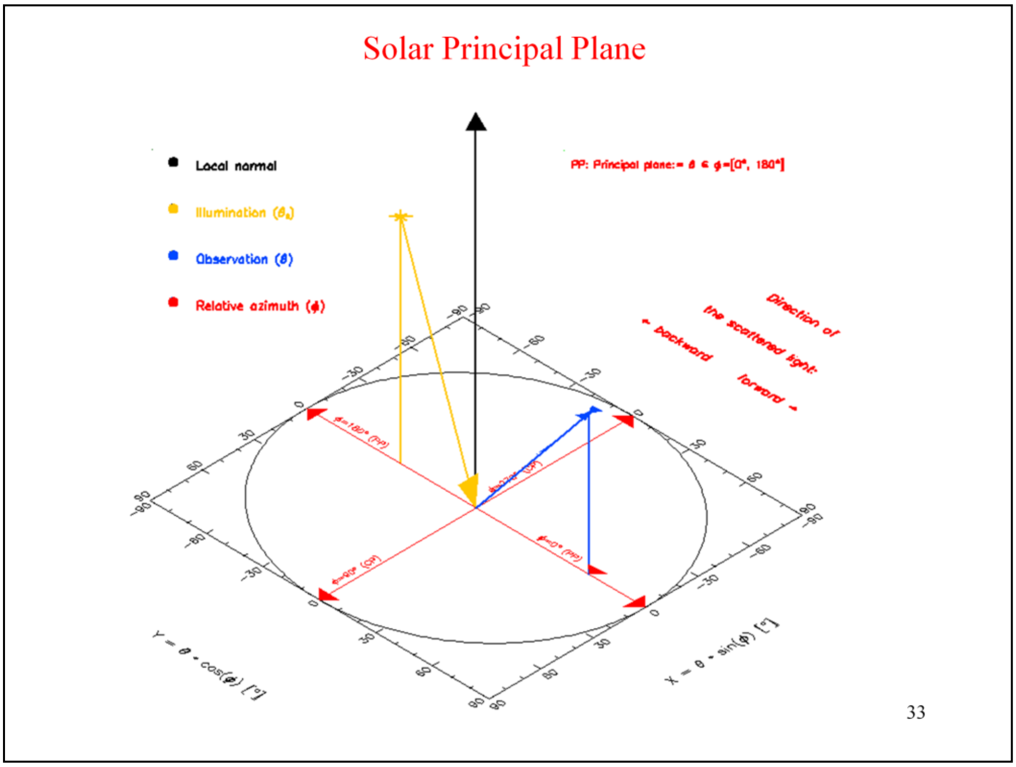

Observations that lie in the same plane as the local vertical and the incoming direct solar radiation are referred to as BRFs in the *principal plane*. Observations along a plane whose azimuth differs by +/- 90 degrees to that of the principal plane are referred to as BRFs in the *orthogonal (or cross) plane*. If the direction of observation coincides with that of the direct solar illumination, no shadows are observed within the target and a BRF maximum known as the*hot spot* effect is observed.

Land Processes: The Medium Resolution Earth Observing Satellites

Landsat series: Multispectral Scanner (MSS) and Thematic Mapper (TM)
SPOT series

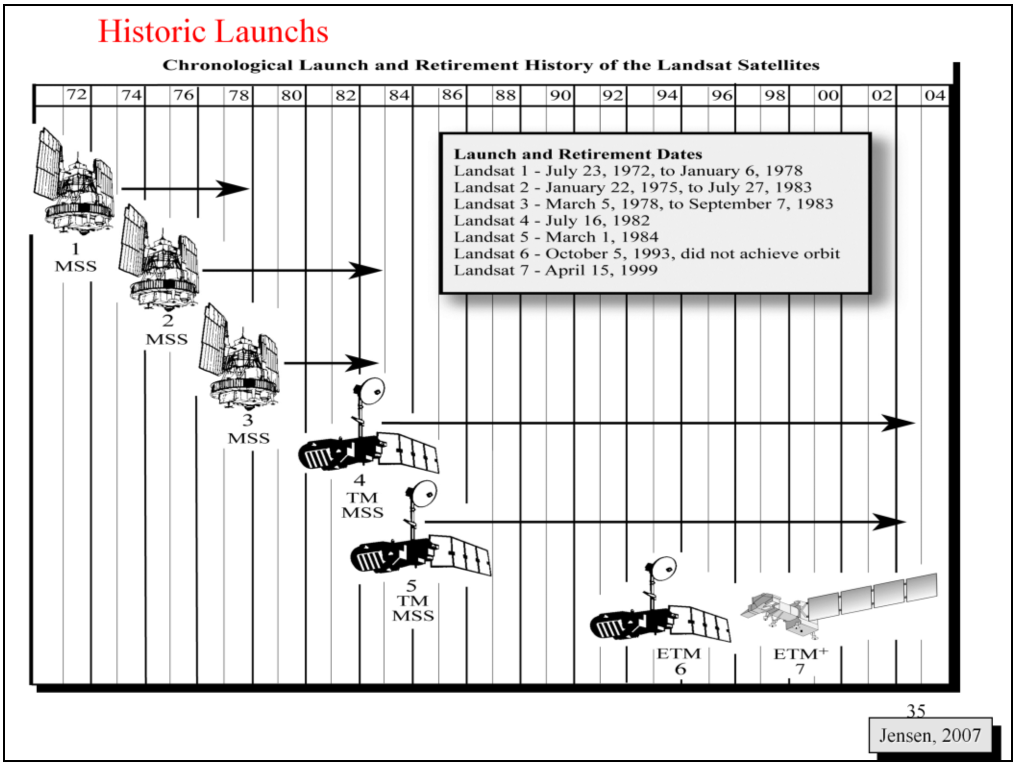

Notice that first three look alike and then next three are similar, than #7 changes again. What does this suggest about the instruments on these platforms?

Landsat I (ERTS): Multispectral Scanner (MSS)

Polar, Sun-synchronous Orbit

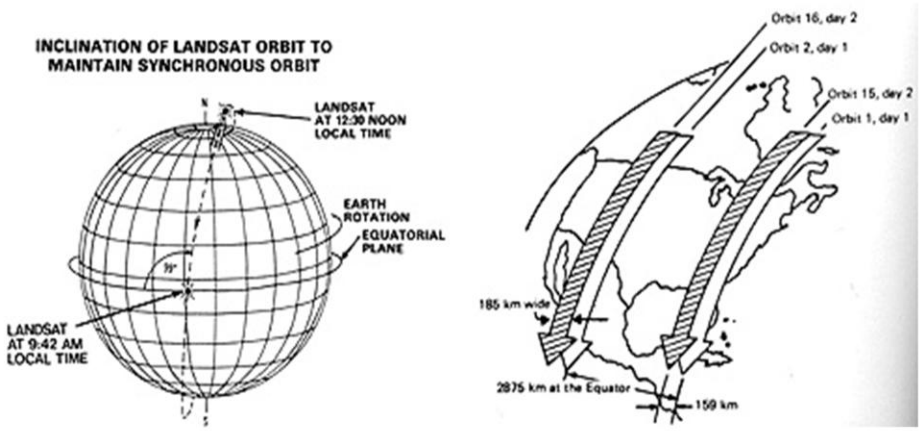

Near Polar, Sun Synchronous, Morning overpass between 9:30-10am
14 passes/day with 103 min. orbit; ~80m pixels swath is 185 km wide

36

The first one to three Landsats orbited at an altitude of 570 miles (923 km);
4 and 5 at 435 miles (705 km).

The orbits of all Landsats are near-polar (inclined 9.09° from a longitudinal line) and Sun-synchronous (pass every time over the equator between 9:30 and 10:00 AM), making 14 passes in descending mode (southward from the North pole in the daylight mode) each day (about 103 minutes for a complete orbital circuit). After any given orbit, the spacecraft will occupy its next orbit some 1775 miles (2875 km) to the west; on the next day, the orbits are so configured so that orbit 15 has displaced westward by 98 miles (159 km) at the equator.

Landsats 1-3 will reoccupy almost precisely the same orbit after 252 such orbits, or 18 days later; Landsats 4 and 5 reoccupy on a 16 day cycle. Under the above orbital conditions, and with an angular field of view if 11.58 ° the width of a Landsat MSS scene is 185 km (114 statute or 100 nautical miles). The continuing orbital strip is cut every 185 km to produce a given image' length. These same frame dimensions hold for the Landsat Thematic Mapper (TM) images.

1 scene: 185 mi x 185 mi = 13,300 sq. miles; 33,225 sq. km; 8,512,000 acres

Orbit Tracks of Landsat 1, 2, or 3 During A Single Day of Coverage

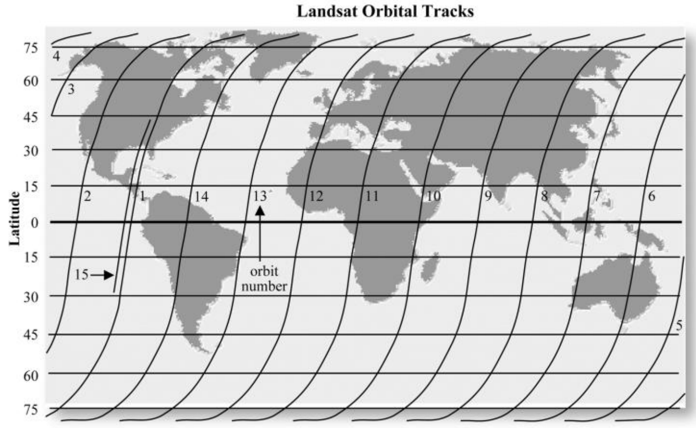

37
Jensen, 2007

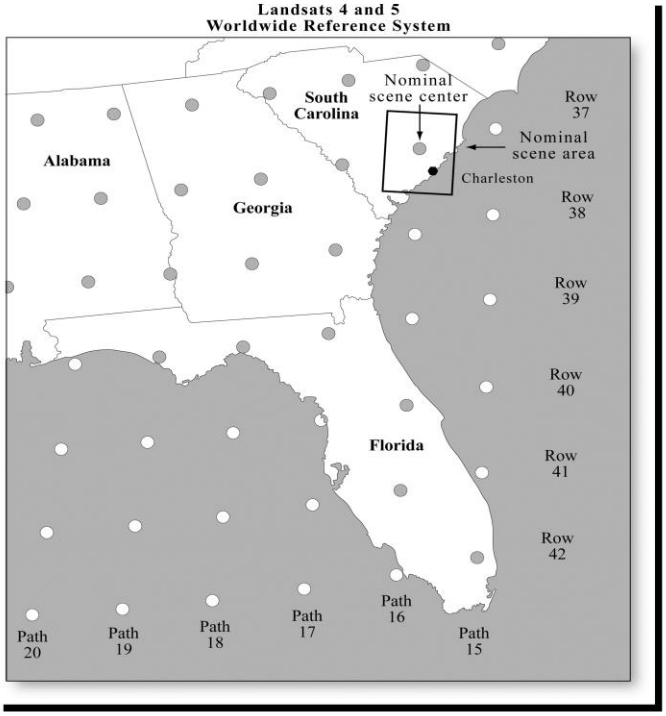

Landsat "scenes" are provided in blocks of 185 km x 185km;

New mode (as of 2009) will let you specify area to be downloaded

Jensen, 2007

38

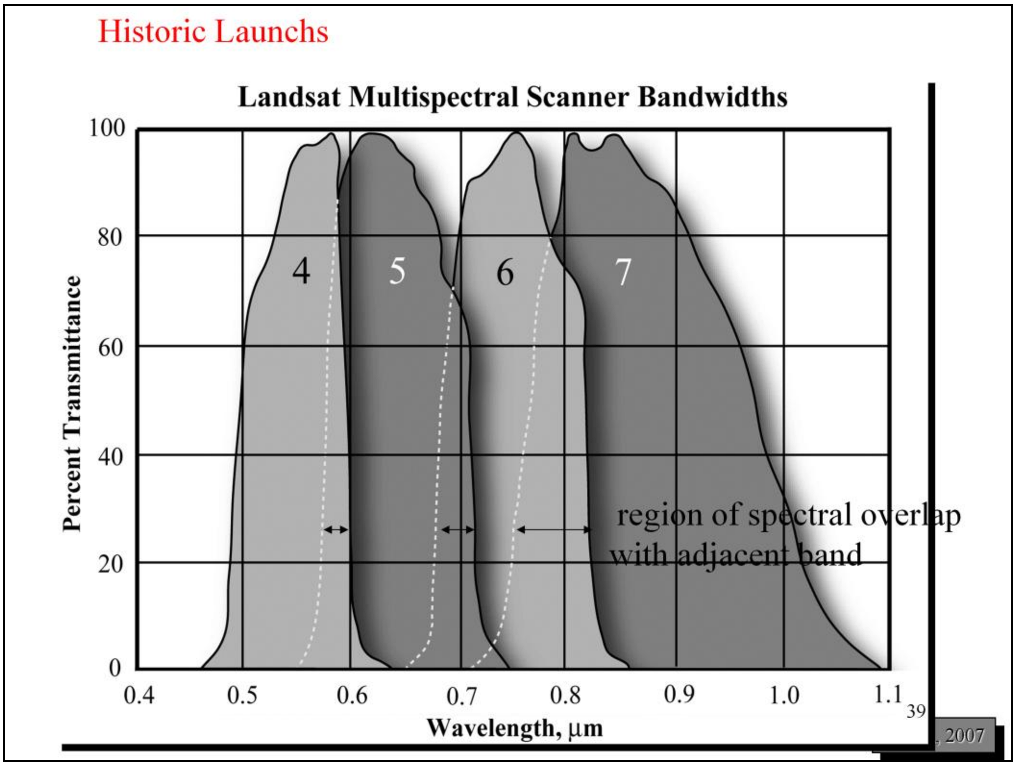

Due to issues with the detector sensitivity and the filters used in fabricating the detector, band passes do not have non-overlapping square-wave structure but are sensitive to some wavelengths more than others and some wavelengths are detected by more than one band.
Newer instruments have less overlap and more Gaussian-shaped sensitivities.

Why are bands called band 4, 5, 6, 7? This is an artifact of how the instruments were designed and earlier bands (not used on MSS) were termed bands 1, 2, 3.

Historic Launchs

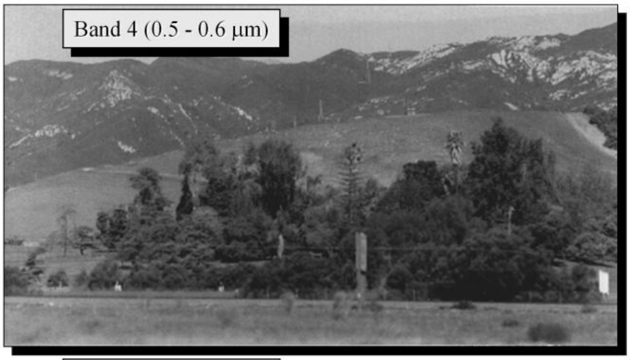

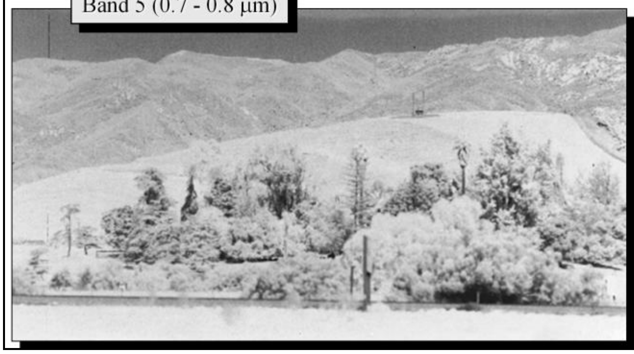

Landsat MSS Terrestrial Images of Goleta, CA Obtained on March 4, 1972

40

Jensen, 2007

Landsat 5 Flight Segment

26 years of on-orbit operations

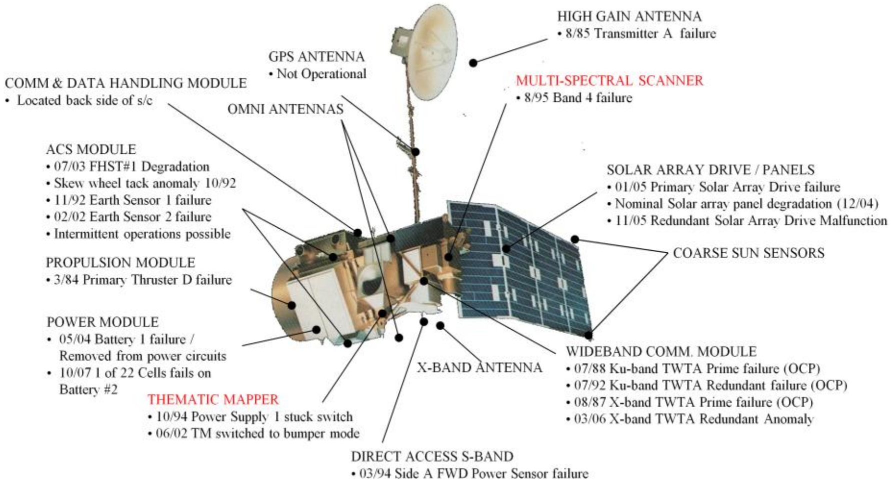

Landsat Multispectral Scanner (MSS) and Landsat Thematic Mapper (TM) Sensor System Characteristics

	Landsat Multispectral Scanner (MSS)			Landsat 4 and 5 Thematic Mapper (TM)		
	Band	Spectral Resolution (μm)	Radiometric Sensitivity (NEΔP)[a]	Band	Spectral Resolution (μm)	Radiometric Sensitivity (NEΔP)
	4[b]	0.5 – 0.6	0.57	1	0.45 – 0.52	0.8
	5	0.6 – 0.7	0.57	2	0.52 – 0.60	0.5
	6	0.7 – 0.8	0.65	3	0.63 – 0.69	0.5
	7	0.8 – 1.1	0.70	4	0.76 – 0.90	0.5
	8[c]	10.4 – 12.6	1.4K (NEΔT)	5	1.55 – 1.75	1.0
				6	10.40–12.5	0.5 (NEΔT)
				7	2.08–2.35	2.4
IFOV at nadir	79 × 79 m for bands 4 through 7 240 × 240 m for band 8			30 × 30 m for bands 1 through 5, 7 120 × 120 m for band 6		
Data rate	15 Mb/s			85 Mb/s		
Quantization levels	6 bit (values from 0 to 63)			8 bit (values from 0 to 255)		
Earth coverage	18 days Landsat 1, 2, 3 16 days Landsat 4, 5			16 days Landsat 4, 5		
Altitude	919 km			705 km		
Swath width	185 km			185 km		
Inclination	99°			98.2°		

[a] The radiometric sensitivities are the noise-equivalent reflectance differences for the reflective channels expressed as percentages (NEΔP) and temperature differences for the thermal infrared bands (NEΔT).
[b] MSS bands 4, 5, 6, and 7 were renumbered bands 1, 2, 3, and 4 on Landsats 4 and 5.
[c] MSS band 8 was present only on Landsat 3.

Jensen, 2007

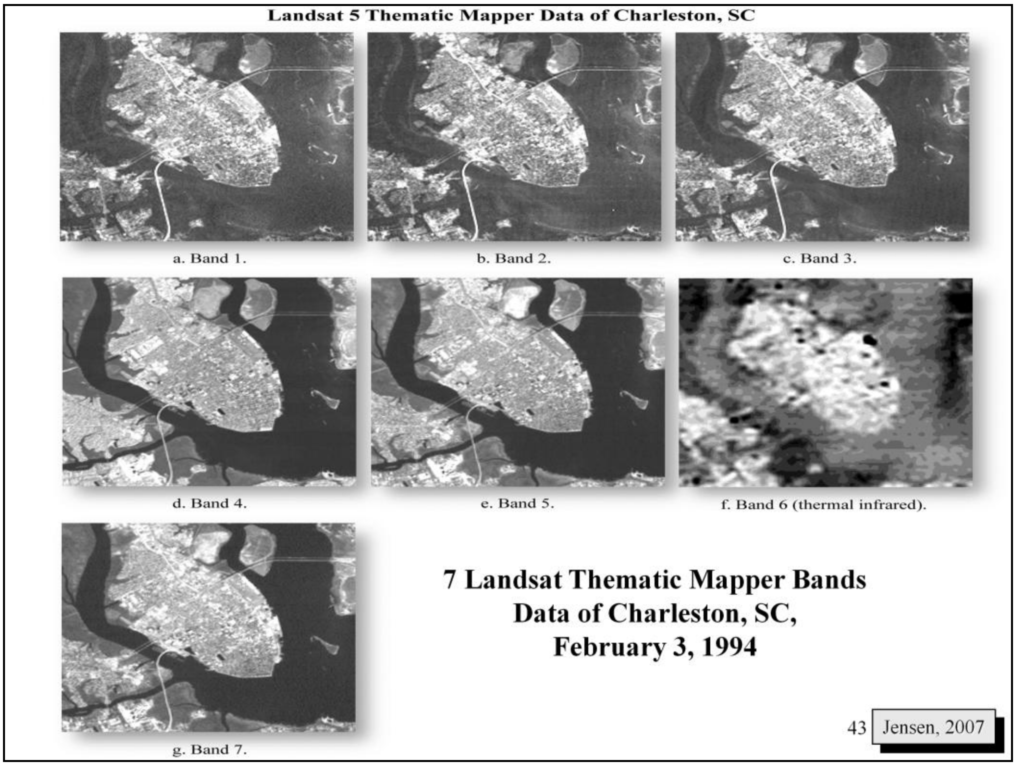

Note: In Landsat TM use, the thermal infrared band is band 6 and the SWIR band is band 7.

Landsat 7 Flight Segment

~11 years of on-orbit operations

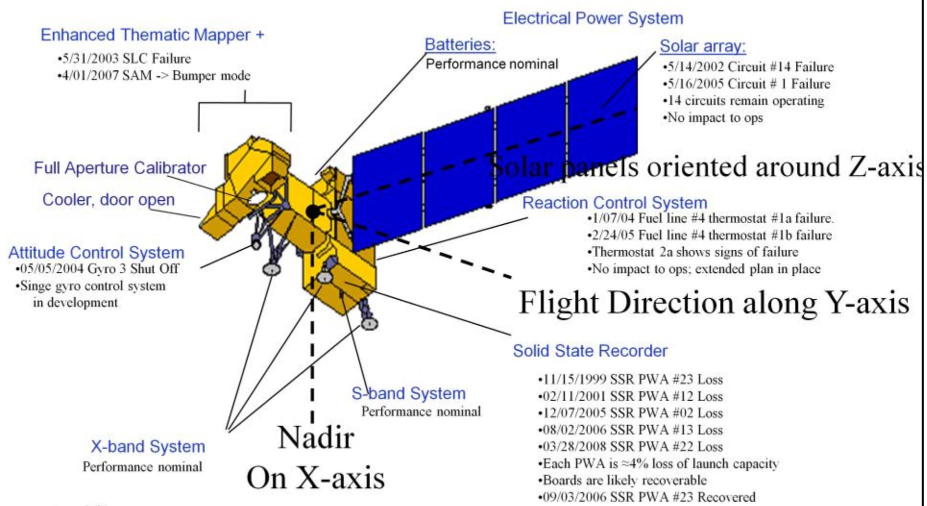

16 day repeat orbits
9:30-10am overpass
30m pixels
(185 X 185) km^2 swaths

What you should know, lecture 4

1. What determines canopy reflectance and how does it differ from leaf reflectance
2. Concept of multiple scattering
3. Relationship between leaf area (or mass) and canopy reflectance
4. How does Red, Near-infrared reflectance change with leaf area?
5. Relevance for detection in different ecosystems
6. Leaf angle impacts on canopy reflectance
7. Orbital, spectral, spatial characteristics of Landsat satellites (MSS and TM instruments).

Introduction to Georeferencing

- Assigns map projection and coordinates to each pixel in a digital image
- By georeferencing an image to a map, we can then georeference other spatially explicit data to the same map for combined use in a GIS.

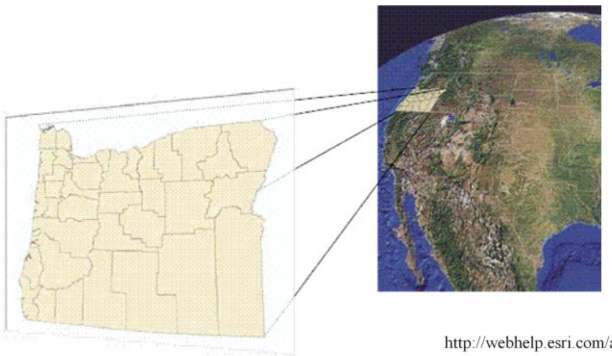

http://webhelp.esri.com/arcgisdesktop/9.2

By establishing a mathematical relationship between the addresses of pixels in an image and the corresponding coordinates of those points on the ground, we can reassign the X and Y values of a given pixel map coordinates such as eastings and northings, or latitudes and longitudes, rather than sample and line numbers

Expressing image pixel addresses in terms of map coordinates is often referred to as geocoding, or georeferencing.

Once an image is georeferenced, we can register other spatial data types, such as geophysical measurements, image data from other sensors using the same mathematical relationships to a map in order to create a georeferenced spatial database which can be used in a GIS.

Sources of Geographic Error

- Radiometric Distortion
  - Atmosphere
  - Instrument
- Geometric Errors
  - Systematic Errors
  - Non-systematic errors

When image data is collected by satellite and airborne sensors, it can contain errors in its geometry and in its pixel brightness. Errors in pixel brightness are referred to as radiometric errors (or distortion), and can result from effects of the atmosphere and errors due to the instrument. We will discuss how to correct for atmospheric effects on Tuesday.

There are more potential sources of geometric distortion that can have more severe effects on our data, especially if we wish to conduct subsequent spatial analysis on our data.

Systematic Error

- Scanning time and Earth rotation
- Panoramic distortion
- Earth's curvature

Line scan and pushbroom sensors require a finite amount of time to acquire a frame of image data. Scan skew is caused by both the forward motion of the platform during the time required for each mirror sweep. Additional distortion is created by the rotation of the earth from west to east as the sensor acquires the image data. If the platform were to change velocity, it could result in along track distortion.

Panoramic distortion is caused by along scan distortion. For scanners used on satellite and aircraft platforms, the angular IFOV is constant, which means that the effective pixel size on the ground is larger at the extremities of the scan than at nadir (directly overhead). This can create compression of image data at the edges. Pixel positions can also be distorted with wide field of view systems. In these systems, the scanner records pixels at constant angular increments, and are displayed in a grid of uniform centers. However, the spacing of the pixels on the ground increases as the scan angle increases. This is the effect of scan angle on pixel size at constant angular instantaneous field of view. However, image data is often compressed which will result in equal-size pixels in a uniform grid. The number of pixels recorded over the outer grid cells in the along track direction will be smaller than those at or near nadir. This distortion is sometime referred to as an s-shaped distortion.

Systematic errors can be corrected using data from the platform ephemeris and knowledge of the internal sensor distortion.

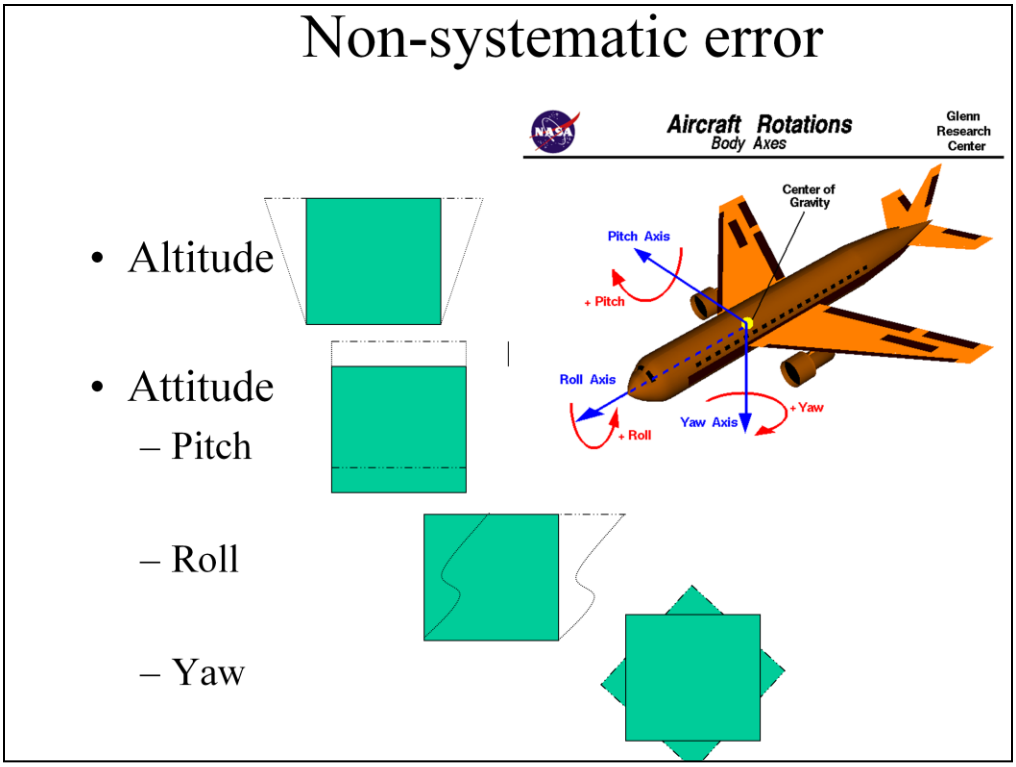

We should be aware of the systematic errors that may distort our data. However, most remote sensing imagery you obtain will already be corrected for these types of systematic errors. Satellites and aircraft collect ephemeris data which is used to apply corrections prior to distribution of data.

Non systematic errors require ground control points in order to correct geometric distortions. A ground control point is a point on the Earth's surface where both image coordinates (measured in rows and columns) and map coordinates (measured in degrees of latitude and longitude, or feet, or meters) can be identified. Geocoding is simply the term used to express a pixel "address" in terms of map coordinates, rather than lines and samples.

Variations in elevation or altitude of a platform can lead to a geometric distortion. Platform attitude is often described in terms of yaw, pitch, and roll during forward travel. The only source for these sorts of distortions in data from satellite platforms would be from orbit velocity variations due to the eccentricity of the earth and the non-sphereicity of the earth.

However, attitude in aircraft platforms play a major role is image distortion, and although ephemeris can be collected from GPS gyro sensors to correct data, ground control points are often needed to further correct the data.

Geocorrection

- Removes internal and external geometric distortion
- Georeferences or geocodes the image
- Two types
  - Image to Map
  - Image to Image

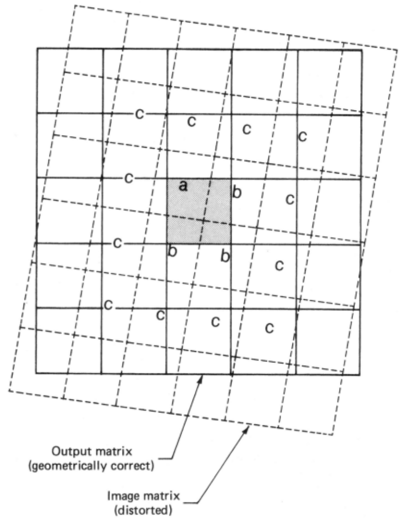

Figure: Lillesand et al., 2005

Geocorrection is what we do to georeference or geocode our image (give it global coordinates) and correct for any distortion that may have been caused by the above factors.

Image to map rectification makes the geometry of an image planimetric. This does not remove the distortion caused to topographic relief.

Image to image registration is the translation and rotation alignment process (or warping) by which two images of like geometry and of the same geographic area are positioned coincident with respect to one another so that corresponding elements of the same ground area appear in the same place on the registered image.

Geometric correction techniques

- Models sources of distortion and establish correction formulae
- Use ground control points (GCPs) to establish a mathematical relationship between your image pixels and correspondent map (or image) coordinates.

Modeling the nature and magnitude of the source of image distortion can be very effective if the type of distortion s well characterized, like for instance, the earth’s rotation (such as many satellite images).

However, more frequently the use of ground control points are used to correct imagery, especially with airborne imagery). The mathematical relationships established between the two images to be registered can be used irrespective of the user’s knowledge of the source and type of distortion.

Image to Map Georegistration: Our Map

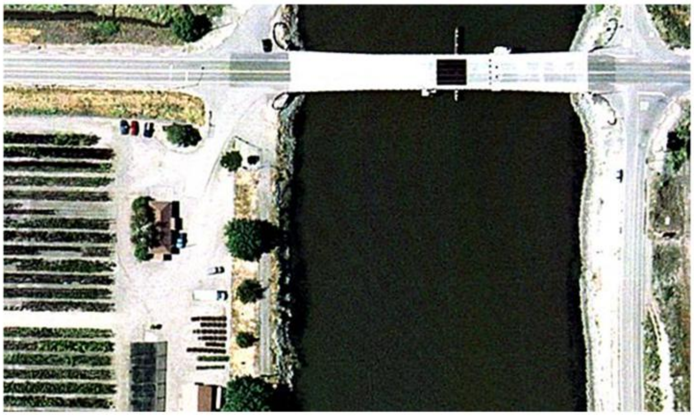

- 2004 USGS Orthorectified 3-band Color Aerial Digital Imagery
- Pixel Size: 0.3m

In order to georegister our HyMap imagery, we will have to first mosaic together 12 orthophotos. An orthophoto is an aerial photo that has been planimetrically corrected to remove distortion in the image from camera tilt, lens distortion, and topographic relief. This means that the scale of the photo is uniform, presumed to be accurate, and is geocoded, so it can be considered a map.

Step 1: Selecting GCPs

- Pick Points that have sharp contrast
  - Building corners
  - Roads neighboring dark fields
  - Bridges on water channels or roads
  - Center of tree crowns
- If working with images from different times, make certain that the points have not changed from one image to another.

Because we are selecting GCPs that will be used to determine the mathematical relationship between the map and the image, it is important to select GCPs that are evenly spaced throughout the image. A general rule for selecting GCPs is that there should be a distribution of control points around the edges of the image to be corrected with a scattering of points over the body of the image.

Examples of GCP Selection

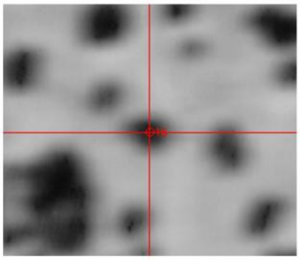

Center

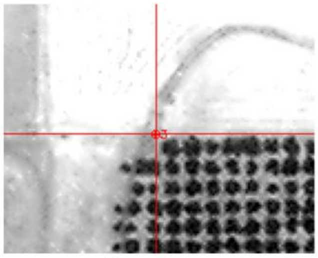

Road Intersections

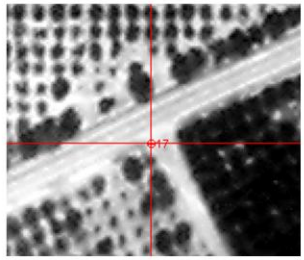

Field Corners

Point 1: Orthophoto

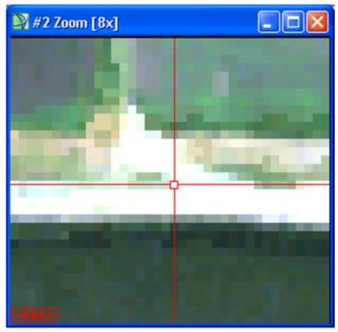

Point 1: HyMap Image

Point 2:

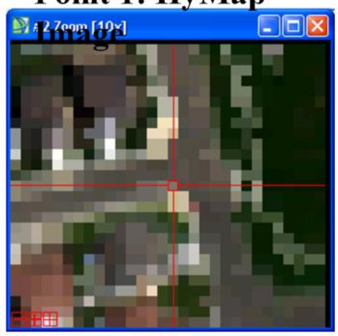

Point 2: HyMap

Step 2: Select Warping Method

- RST (Rotation, scaling, and Translation)
- Polynomial
- Delauney Traingulation

$$x = a_1 + a_2 X + a_3 Y$$

$$y = b_1 + b_2 X + b_3 Y$$

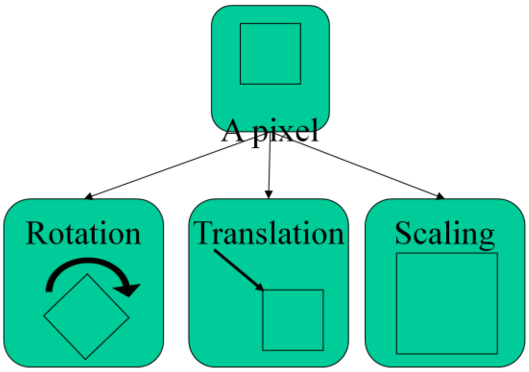

RST: Rotation, Scaling, and translation is the simplest and fastest warping method. This method needs a minimum of three or more GCPs. It uses an affine transformation which preserves the collinearity between points (three points on a line will continue to be on the line after a transformation), and maintains the ratio of distance between a line.

It generally is composed of a linear combinations of two transformations (rotation, and scaling), and a shift (translation).

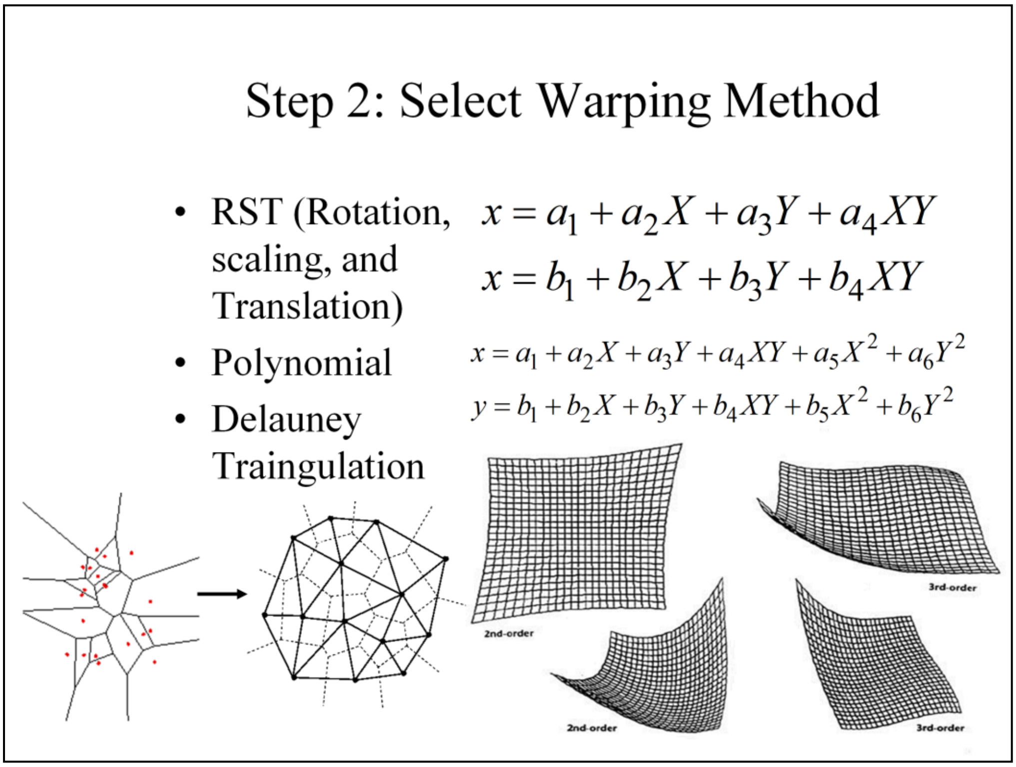

RST does not account for image shearing (our square pixel is distorted to look like a parallelogram). A first order polynomial warp includes and XY interaction term to account for image shear.

In general, I first-order polynomial warp will return more accurate results than RST, with a tradeoff in the amount of processing time required.

Polynomial warping is available from the 1st to the nth degree. The degree available is dependent upon the number of GCPs selected where #GCPs > (degree +1)$^{2.}$

As stated earlier, 3 GCPs is the minimum for both RST and first-order polynomial mapping. What is the minimum number of GCPs needed for 2nd order polynomial mapping? (ans=6). How about third order mapping? (ans=10).

In practice however, significantly more GCPs than this are selected, and the coefficients are evaluated using a least squares estimation. By using a lot of GCPs, one GCP that contains significant positional error either on the map or the image will not have an undue influence on the polynomial coefficients.

Delauney triangulation fits triangles to irregularly spaced GCPs and interpolates values to the output grid. This approach does not take a pixel-by-pixel approach. It is sometimes visualized as a rubber sheeting approach to image warping.

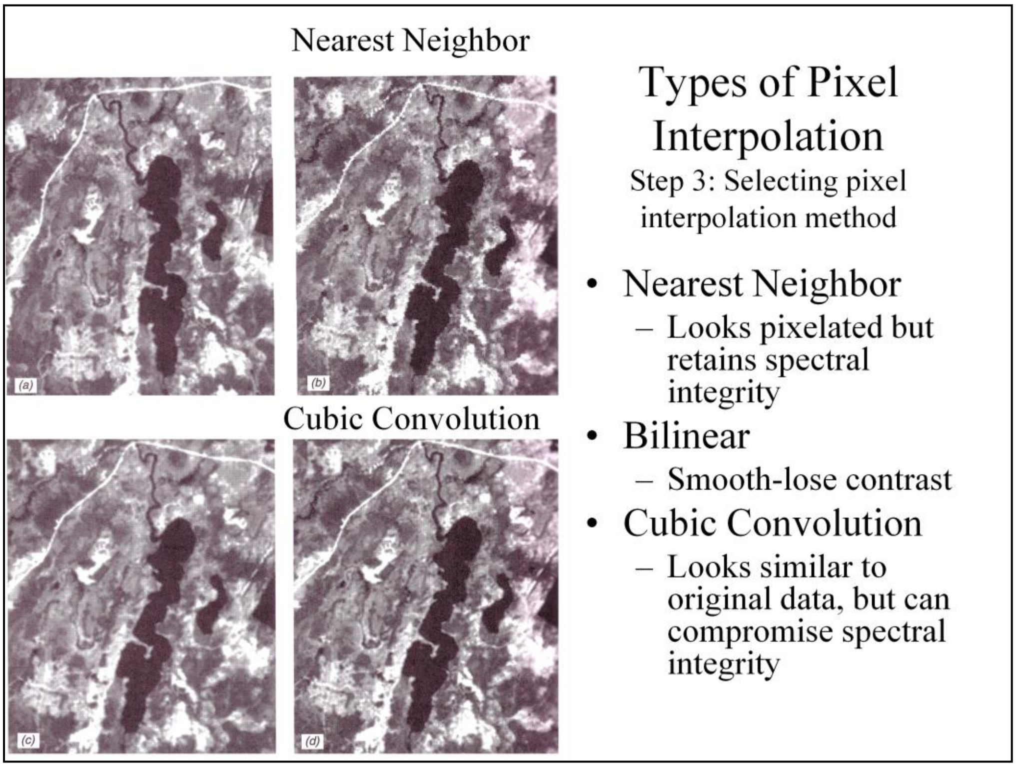

When you project a registered pixel, the exact pixel center is not going to fall in exactly the same place as the image. There are three techniques used to determine what the new pixel’s brightness is going to be.

Nearest neighbor sampling simply chooses the actual pixel that has its center nearest the point located in the image. This is often the preferred technique because it maintains the pixel’s original brightness, and simply rearranges it into a position that gives it correct geometry.

Bilinear interpolation uses three linear interpolations over the four pixels surrounding the point in an image corresponding to a given grid position.

Cubic convolution interpolation uses the surrounding sixteen pixels, and yields an image product that is smooth in appearance, but with altered pixel brightness.

Accuracy of Georegistration

- RMS Error (Root Mean Squared Error), similar to standard deviation, for a small sample size estimates that there is a 40% chance of the points are associated with the original position.

- The **root mean squared error** of an individual GCP point is evaluated by the equation:

- RMS error = $$\sqrt{\frac{\sum_{i=1}^{n}\left((x_i - \hat{x}_i)^2 + (y_i - \hat{y}_i)^2\right)}{n}}$$

- Where x_i and y_i are the original row and column coordinates for the GCP in the image and $\hat{x}_i$ and $\hat{y}_i$ are the computed or estimated coordinates in the original image. By dividing by n to take the mean of the sum of square error.

Today:

- Open georeg tracking info spreadsheet, and complete it as you work.
- Begin working through Lab exercises 2 & 3.